ISSN: 2692-5397
DOI: 10.33552/MCMS.2024.06.000632
Modern Concepts in Material Science
Iris Publishers

Research article

Immobile Charges Play an Essential Role for Membrane Potential Generation

Hirohisa Tamagawa[1]*, Bernard Delalande[2], Wenyi Lin[3] and Minoru Sasaki[1]

[1]*Department of Mechanical Engineering, Gifu University, Japan*

[2]*Freelance, France*

[3]*Kawamura Electric Inc., 3-86, Akatsukicho, Seto-City, Aichi-Pref, Japan*

***Corresponding author:** Hirohisa Tamagawa, Department of Mechanical Engineering, Faculty of Engineering, Gifu University, 1-1 Yanagido, Gifu, Gifu, 501-1193, Japan

Received Date: May 22, 2024

Published Date: June 13, 2024

Abstract

The physiological mechanism of membrane potential generation relies on the passage of mobile ions across the plasma membrane, which is selectively permeable to mobile ions. The existence of a membrane and the transport of ions across it are essential for the generation of membrane potential. However, a long-forgotten theory, Association-Induction Hypothesis, asserts that the heterogeneous distribution of charges in space, because of the localized charges of heterogeneously distributing ions due to the ion adsorption/desorption, is the true cause of membrane potential generation. Using an artificial living cell model consisting of a viscous aqueous solution, the mechanism of membrane potential generation is restudied in this work. The results indicate that membrane potential can be generated even in the absence of a plasma membrane and that ion adsorption leading to a heterogeneous spatial charge distribution is an essential factor for membrane potential generation. Consequently, the authors invite people to reconsider the Association-Induction Hypothesis as a genuine mechanism for generating membrane potential.

Keywords: Membrane potential; Membrane theory; Association-Induction Hypothesis; membrane permeability; Ion adsorption

Abbreviations: PVA: polyvinyl alcohol; AIH: Association-Induction Hypothesis; IER: Ion-Exchange Resin; AER: Anion-Exchange Resin (DOWE X, Cl form, Dow Chemical Company, Michigan, USA); CER: Cation-Exchange Resin (DOWE X, H form, Dow Chemical Company, Michigan, USA); IEM: Ion-Exchange Membrane; AMV: Selemion AMV (anion exchange membrane manufactured by Asahi Glass Co., Ltd.); CMV: Selemion CMV (cation exchange membrane manufactured by Asahi Glass Co., Ltd.); GHK eq. Goldman-Hodgkin-Katz equation

Introduction

The cell potential, called the membrane potential, has been studied for decades. Today, all textbooks describe that passive and active transmembrane ion transport governed by ion channels and sodium pump is responsible for the generation of membrane potential [1,2]. This is called membrane theory. The plasma membrane is an essential element in the generation of membrane potential. In fact, it is widely accepted that ion transporters, such as ion channels and sodium pumps, are integrated into the plasma membrane. The absence of a plasma membrane means the absence of these ion transporters (ion channels and sodium pump). Consequently, the absence of the plasma membrane means that the membrane potential is an unimaginable event. However, it has been repeatedly reported that membrane potential-like potentials are observed in various artificial systems that do not contain ion transporters. Therefore, the mechanism of membrane potential generation remains a controversial topic in some research groups.

The Association-Induction Hypothesis (AIH) is a long-forgotten physiological theory proposed by the late Gilbert Ling [1-3]. AIH suggests that the membrane potential can be generated without ion transport across the plasma membrane. The key factor in generating the membrane potential is the heterogeneous spatial distribution of the ions caused by ion adsorption. Charges of ions inevitably generate potentials around them. Superimpose of these potentials are observed as the membrane potential in a living cell. The heterogeneous ion distribution inevitably results in a heterogeneous potential circumstance, regardless of whether the system in question is a living cell or an artificial system. This is merely a consequence of electromagnetism. Consequently, no ion channels or pumps are required for the generation of membrane potential from living cells. In fact, one of the authors of this article, Tamagawa, previously successfully derived a membrane potential formula using the AIH [4,5]. AIH is a quite comprehensive physiological theory that is applicable for theorizing the potential characteristics of both living and nonliving systems. At this moment, there is no rational reason to rule out AIH as the mechanism of membrane potential generation of living cells, though AIH contradicts the currently widely accepted membrane theory. This work was carried out with the aim of disproving the membrane theory and proving that ion adsorption is the mechanism of membrane potential generation, as suggested by the AIH.

Theory

First, two conflicting mechanisms of membrane potential generation – the membrane theory and the Association Induction Hypothesis (AIH) – are detailed here.

Membrane Theory and Some Experimental Observations Contradicting It

Membrane theory is the best-known and most widely accepted physiological theory. It states that membrane potential is caused by transmembrane ion transport governed by ion transporters called ion channels and pumps. This mechanism is intuitively well understood and even mathematically formulated with precision [6-8]. The Goldman-Hodgkin-Katz equation (GHK eq.) is a typical example. Eq. 1 is an example of a GHK equation.

$$\phi = -\frac{kT}{e}\ln\frac{P_{Na}\left[Na^{+}\right]_{in} + P_{K}\left[K^{+}\right]_{in} + P_{Cl}\left[Cl^{-}\right]_{out}}{P_{Na}\left[Na^{+}\right]_{out} + P_{K}\left[K^{+}\right]_{out} + P_{Cl}\left[Cl^{-}\right]_{in}} \quad (1)$$

P_i *(i = Na⁺, K⁺, Cl⁻)* is the permeability of the membrane to mobile ions. If the membrane is impermeable, $P_i = 0$. Then, the GHK eq. of Eq. 1 collapses [1,6-8]. Therefore, the GHK eq. states that the membrane potential is unthinkable unless the membrane is permeable. Now what if the membrane is freely permeable to any mobile ions? Free ions would eventually distribute equally everywhere, which is represented by $[Na^+]_{in} = [Na^+]_{out}$ $[K^+]_{in} = [K^+]_{out}$ $[Cl^-]_{out} = [Cl^-]_{in}$ Therefore, ϕ of Eq. 1 would result in zero potential, but the ions never evenly distribute in the real living cell. The membrane theory states that the sodium-potassium pump is one of the key players in achieving the disparity between the concentrations of extracellular and intracellular ions [1,2,9]. The pump functions by consuming the energy of ATPs and maintaining the ion concentration gradient across the membrane. Therefore, the disparity between the intra- and extra-cellular ion concentrations is one of the proofs that the cell is in the living state. The GHK eq. of membrane theory is a quite effective tool for reproducing the membrane potential quantitatively. Even the complex dynamics of the membrane potential, the so-called action potential, is quantitatively well associated with the GHK eq. on the ground that the potential variation is due to the variation of P_i [10-14]. The variation of P_i is physiologically attributed to the variation of the degree of functionality of the ion transporters [15,16]. Namely, the role of the ion transporter is ingeniously incorporated into the GHK eq. as P_i in the GHK eq. (see Eq. 1). Although significant efforts have still been made even today to develop theories that accurately predict membrane potential [12,17,18], the foundations of membrane theory have remained solid for decades. In fact, researchers in classical physiology recognized that the existence of ion channels had been predicted and then experimentally discovered [1,2,19]. This is the most important triumph of membrane theory. The discovery of the sodium pump is also another well-known proof of the support for membrane theory [1-3,20,21]. Currently, virtually no one has questioned the membrane theory. However, it has been known that even nonliving systems containing no ion transporters can generate the action potential.

Fox had been involved in the investigation of the electrical characteristics of the proteinoid microsphere [22-26]. Fox's microsphere is not a living system, and it does not contain any ion transporter. However, it exhibited a potential that is indistinguishably similar to the action potential of living cells. In fact, action-potential-like potentials are observed in various non-living systems. For example, Yoshikawa et al. observed the oscillatory potential generated across an artificial membrane that separates two electrolytic solutions [27-33]. Flasterstein reported a spontaneous fluctuation of the potential at the metal-electrolytic solution interface, which is a non-living system, although the magnitude of the potential is quite small compared to the membrane potential of a living cell [34,35]. Therefore, potential changes with time in electrolytic solution systems must naturally occur regardless of whether the system in question is a living system or not. One may think that one needs to consider living systems and non-living systems separately and independently. However, for example, the GHK eq. never distinguishes the living systems from the nonliving systems. In the derivation process of GHK eq., we do not have to use any constraint that the concept of GHK eq. is applicable only to living systems [7]. However, non-living systems can generate the membrane potential-like potential as mentioned above. These matters inevitably give us the impression that membrane theory is wrong or at least incomplete. Relating this thought, we would like to show one of Ling's works, called the EMOC experiment (effectively membrane-pumpless open-ended cell), which is quite suggestive for this work [1,36]. A frog muscle was suspended vertically. The lower end of this muscle had the cut end and the cut end was exposed to the electrolytic solution containing K^+ and Na^+. Since the cut end was not covered by the plasma membrane, the channels and pumps were not in contact with the solution containing K^+ and Na^+. He maintained this ex-

perimental state for tens of hours and found that the intracellular level of K^+ increased rapidly over time, while that of Na^+ did not. The disparity between the extracellular and intracellular ion levels can be achieved even in the absence of the ion transporters. The ion disparity of living cells may not be a consequence of the functionalities of ion transporters. We may have to reconsider the origin of the membrane potential from the clean slate.

Association-Induction Hypothesis (AIH)

The Association-Induction Hypothesis (AIH) is a theory completely different from the membrane theory. According to the AIH, the membrane potential is generated by the heterogeneous spatial distribution of the charges as a result of ion adsorption. It is explained in detail here using Figure 1. Assume that the mobile cations and anions are homogeneously distributed, as shown in Figure 1(a). Because of the homogeneity of the charge distribution, the potentials generated by the positive charges of the cations and negative charges of the anions cancel each other out, and a homogeneous potential is formed everywhere. On the other hand, once immobile charges, such as electrolytic polymer chains bearing anions, are introduced into the cell as illustrated in Fig. 1(b), the immobile anion adsorbs the mobile cation and their charges become neutralized. However, some of the immobile anions on the fixed polymer chains remain unadsorbed with cations because of the mass action law. Therefore, the cell contains anions in the mobile and immobile states, although the cell contains mobile cations only. This heterogeneous state of the ion distribution results in a totally different potential than the cell potential when the ions distribute homogeneously, as illustrated in Figure 1(a) (A more mathematical treatment about potential generation in aqueous solution systems containing immobile charges and mobile charges is given in ref. [37]). This is the membrane potential based on AIH. This AIH-based explanation is just the idea of electromagnetism and thermodynamics in basic physics.

The degree of heterogeneity of the ion distribution depends on the degree of ion adsorption. Consequently, ion adsorption governs the membrane potential. The living cell is full of proteins and lipids that carry immobile charges, and these immobile charges can serve as adsorption sites for mobile ions. Adsorption (or desorption) can occur wherever there are adsorption sites for mobile ions. Therefore, the AIH asserts that membrane potential generation does not require the transport of ions across the plasma membrane and that even ion channels and pumps are not necessary [1-3]. Ion adsorption is not a phenomenon limited only to living systems.

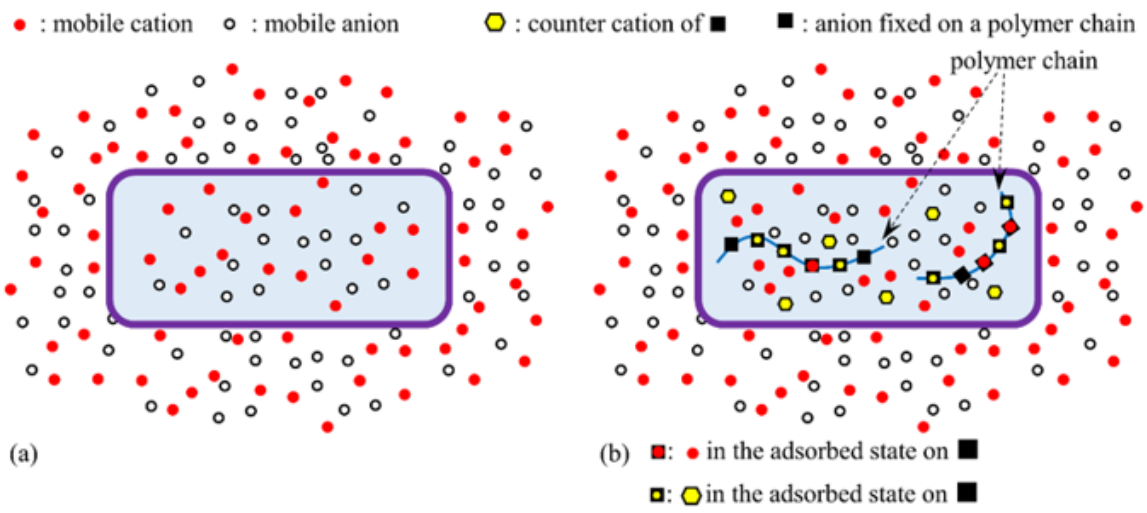

Figure 1: Ion distribution in a cell (a) homogeneous ion distribution (b) heterogeneous ion distribution due to the adsorption of cations on the anions of the polymer chains.

From a theoretical point of view, ion adsorption is governed by the mass action law, and it takes place in various non-living systems. The mass action law is utilized in various applications, and water purification using ion exchange resin is a good example. Ion adsorption takes place in the living cell, and scientists often discuss ion adsorption even within the range of the membrane theory [38-40]. Namely, the physiologists, of course, do not deny the occurrence of the ion adsorption in the living cell. However, when the membrane potential is computed theoretically and numerically, the ion adsorption facet is completely missing in the formula. For example, the GHK eq. does not contain any term that takes into consideration ion adsorption. Similarly, the influence of charges, which can vary by the adsorption among ions, on the potential generation is disregarded in the GHK eq., too. Physiologists often discuss the influence of these effects (ion adsorption and charge) on potential generation, but have never successfully associated them with a potential formula such as the GHK eq. In the old days, Ohki discussed the membrane potential taking into account the membrane sur-

face charge effect [38]. But he did not deny the membrane theory, though he did not provide any explicit formula in which the charge influence on the membrane potential is incorporated and, at the same time, which is in line with the membrane theory mathematically. Banarroch et al. discuss the dynamics of membrane potential from various aspects [41]. They stressed the fundamental importance of the consideration of charge separation effect on membrane potential generation, though they did not abandon membrane theory. Hughes approaches the membrane potential study from a new angle [42]. He attempted to integrate both the influence of conventionally considered ion diffusion and the influence of charge on the membrane potential though he has yet to show us any explicit potential formula. His work may drastically change the theoretical treatment of membrane potential generation. The AIH is based on the principle of physics. It does not require the existence of ion channels or pumps. Only the basic principles of physics are required. To date, a small number of researchers have performed this kind of physics-based theorization of the mechanism of membrane potential generation without ion transporters [21,43-52]. They believe that physiology should exist alongside physics. How can we ignore physiology based on physics and how can we support physiological study in the absence of physics? We performed the investigation on the membrane potential mechanisms in mind both the membrane theory and the AIH.

Experiments and the Ideas Behind Them

The protoplasm is viscous in nature. The idea of the protoplasm as an ordinary highly fluidic electrolytic solution would idealize the living cell system too much. By treating the living cell in this way, we could miss out on the fundamental nature of living cells. Not only protoplasm, but also the various facets of a living cell must be over-idealized in today's physiology. A realistic view of the living cell must be necessary to truly theorize the characteristics of the living cell [1,2,20,21,43-53]. The authors of this paper therefore decided to focus on the viscous aqueous solution as an experimental model of protoplasm. The authors measured the potential of viscous aqueous solutions to elucidate the mechanism of membrane potential generation. In Section 4.1, the potential characteristics generated by the interaction between immobile charges and mobile charges (K^+ and Cl^-) in highly fluid electrolytic solution were investigated. In Section 4.2, basically the same experiments described in section 4.1 were performed, but the highly viscous aqueous solution containing PVA was used in place of the highly fluidic solution. In section 4.3, the influence of the existence of a membrane that carries immobile charges (ion exchange membrane) on the generation of solution potentials is discussed. In Section 5.1, the influence of the interaction between the highly viscous charged solution and the mobile ions on the generation of potential in the absence of the membrane was studied, while the same potential characteristics were investigated in the presence of the membrane in Section 5.2. The primary points of the experimental setup and material used in the above-described experiments are summarized in Table 1. The experimental procedure is also detailed in the individual experimental sections.

Table 1: Experimental setup and materials used.

Exp.#	setup	solution[1]	additives	membrane	procedure
Exp. 1	Fig. 2	DI[2]	10^{-4}, 10^{-1} M KCl[8]	none	Table 2
Exp. 2	Fig. 2	DI	10^{-4} M KCl, CER[9]	none	Table 3
Exp. 3	Fig. 2	DI	10^{-4} M KCl, AER[10]	none	Table 4
Exp. 4	Fig. 2	PVA[3]	10^{-4}, 10^{-1} M KCl	none	Table 5
Exp. 5	Fig. 2	PVA	10^{-4} M KCl, CER	none	Table 3
Exp. 6	Fig. 2	PVA	10^{-4} M KCl, AER	none	Table 4
Exp. 7-1	Fig. 17	two PVAs[4]	10^{-1} M KCl, AER	AMV[11]	Table 6
Exp. 7-2	Fig. 17	two PVAs	10^{-1} M KCl, AER	CMV[12]	Table 6
Exp. 7-3	Fig. 17	two PVA	10^{-1} M KCl, CER	AMV	Table 6
Exp. 7-4	Fig. 17	two PVA	10^{-1} M KCl, CER	CMV	Table 6
Exp. 8	Fig. 2	gelatin[5]	10^{-1} M KCl	none	Table 7
Exp. 9	Fig. 2	PVA	10^{-1} M KCl	none	Table 7
Exp. 10	Fig. 17	gelatin	10^{-1} M KCl	AMV/CMV	Table 7
Exp. 11-1	Fig. 17	L[6]: gelatin, R[7]: PVA	10^{-1} M KCl	DM[13]	Table 7
Exp. 11-2	Fig. 17	L: PVA, R: gelatin	10^{-1} M KCl	DM	Table 7

1. the solution that fills the container of the experimental setup
2. deionized water
3. 16wt% aqueous solution of PVA

4. two 16 wt% PVA aqueous solutions
5. 16wt% aqueous gelatin solution
6. left phase of the setup
7. right phase of the setup
8. 10^{-4} M and/or 10^{-1}M KCl aqueous solution
9. cation exchange resin particles
10. anion exchange resin particles
11. anion exchange membrane called Selemion AMV (Asahi Glass Co., Ltd, Tokyo)
12. cation exchange membrane called Selemion CMV (Asahi Glass Co., Ltd, Tokyo)
13. dialysis membrane permeable to mobile ions and water and impermeable to PVA and gelatin

Potential Characteristics of The Electrically Neutral Viscous Solution Systems

Potential in Aqueous Solution Without PVA

Exp.1 Potential Generated by the Addition of KCl Solution

Figure 2 represents the experimental setup. The container of this setup is filled with a solution. Two Ag/AgCl electrodes (an indicator electrode and a reference electrode) are placed in the solution with a 6.5 cm gap between them. The potential generated between the two electrodes was measured as a function of time following the experimental procedure summarized in Table 2. Figure 3 shows the time dependence of the potential generated between the indicator and reference electrodes (see Figure 2). Although momentary potential perturbations were observed when the KCl solution was dropped close to the electrodes, the potential remained basically at 0 V. According to membrane theory, selective ion transport across the plasma membrane is responsible for generating a non-zero membrane potential. In this experiment, Exp.1, no ion-selective membrane was used. Therefore, the non-zero potential cannot be expected at all. Therefore, the observation of the experimentally observed zero potential is in perfect agreement with the membrane theory. However, at the same time, the zero potential is explicable by the AIH since no heterogeneity of ion distribution is expected due to the occurrence of no ion adsorption.

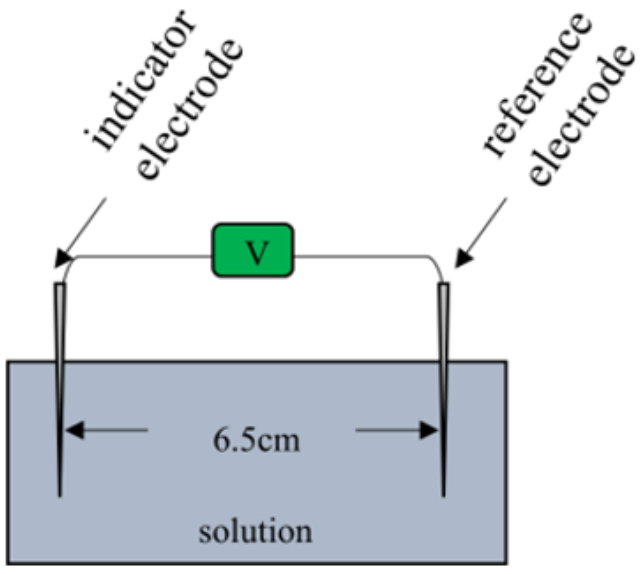

Figure 2: Experimental setup for measuring the solution potential.

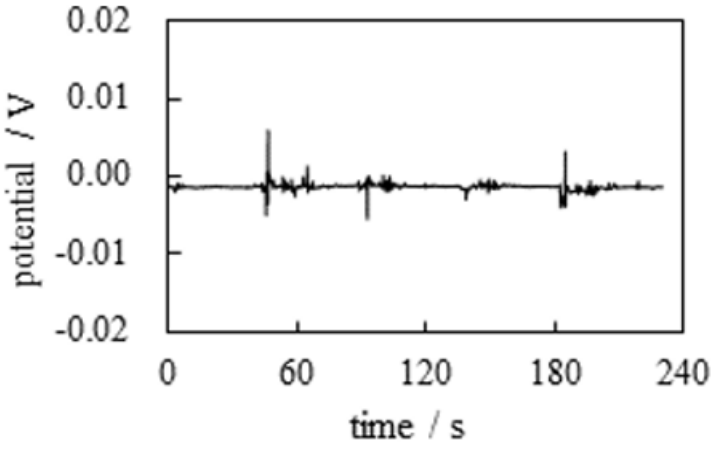

Figure 3: Exp.1 Time dependence of the potential between the indicator and the reference electrodes.

Table 2: Procedure of potential measurement.

t†1 / s	operation†2
0	onset time of the potential measurement
45	addition of a few drops of 10^{-4} M KCl solution near the indicator electrode
90	addition of a few drops of 10^{-1} M KCl solution near the indicator electrode
135	addition of a few drops of 10^{-4} M KCl solution near the reference electrode
180	addition of a few drops of 10^{-1} M KCl solution near the reference electrode

† 1 t: time

† 2 The solution that fills the container of the experimental setup is deionized water.

Exp.2 Potential generated by the addition of Cation Exchange Resin

The same potential measurement as Exp.1 was performed according to the experimental procedure summarized in Table 3. In this measurement, the Cation-Exchange Resin solution was used, which is the mixture of Cation-Exchange Resin (DOWE X, H form, Dow Chemical Company, Michigan, USA) and deionized water (see Figure 4). Figure 5 shows the potential vs. time (see Figure 2) under the experimental condition in Table 3. There is no ion-selective membrane between the indicator and reference electrodes. However, the negative potential was clearly observed after t = 90 s. This non-zero potential cannot be explained by membrane theory. However, the characteristics of this potential can easily be explained by electromagnetism. There were K^+ and Cl^- near the indicating electrode after t = 45 s, but the total charge of K^+ and Cl^- is undoubtedly zero, and these ions are in the thermal motion state. Consequently, the zero potentials generated by the individual ions are canceled, giving zero even after adding KCl at t = 45 s (see Figures. 6(a) and (b)). However, the Cation Exchange Resin solution (CER solution) added in the vicinity of the indicator electrode at t = 90 s is a powdery macroscopic solid (see Figure 4(c)), and the CER dissociates into a mobile cation and an immobile anion, as shown in Figure 6. The non-zero potentials generated by these mobile cations are largely canceled out by the potentials of all other mobile anions in thermal motion. However, the negative charges on the CER are virtually immobile because the CER is a visibly large particle. These charges cannot be fully neutralized according to the law of mass action [54]. The quantity of adsorbed ions on the CER determines the quantity of immobile charges on the CER. It means that the heterogeneity of spatial ion distribution is governed by the ion adsorption/desorption. Therefore, a negative potential is generated in the vicinity of the indicator electrode. Consequently, the negative potential is generated after t = 90 s. The addition of 10^{-4} M KCl near the reference electrode at t = 135 s did not cause the potential change till t = 180 s. It is due to the same reason for the occurrence of no potential change from t = 45 s through t = 90 s. The potential began to increase when CER was added near the reference electrode at t = 180 s. This phenomenon can be explained for the same reason that was used to explain the potential drop at t = 90 s. That is, the potential drop at t = 180 s is due to immobile negative charges of the CER added near the reference electrode, as illustrated in Figure 7. This is in full line with the AIH prediction.

Table 3: Procedure of potential measurement

t†1 / s	operation†2
0	onset time of the potential measurement
45	addition of a few drops of 10^{-4} M KCl solution near the indicator electrode
90	addition of a few drops of CER solution†3 near the indicator electrode
135	addition of a few drops of 10^{-4} M KCl solution near the reference electrode
180	addition of a few drops of CER solution†3 near the reference electrode

† 1 t: time

† 2 The solution in the container of the set-up (see Fig. 2) is a deionized water.'

† 3 CER solution: The mixture of CER and deionized water

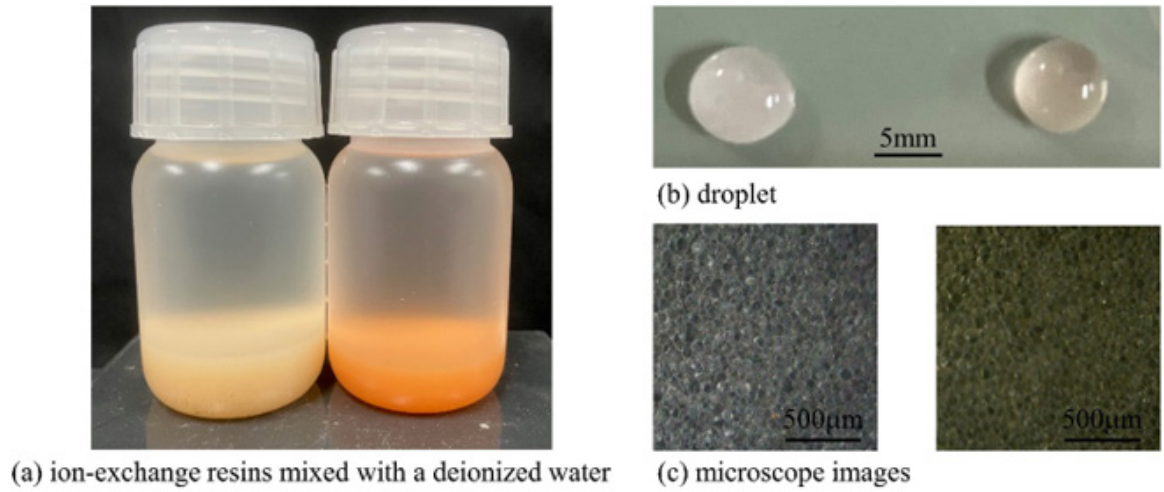

Figure 4: Ion-Exchange Resins (IERs) {Cation-Exchange Resin (CER) in a deionized water (DI) and Anion-Exchange Resin (AER) in a deionized water (DI)} (a) Left bottle: CER in a DI, Right bottle: AER in a DI (b) Left droplet: CER in a DI, Right droplet: AER in a DI (c) Left photo: CER in a DI, Right photo: AER in a DI

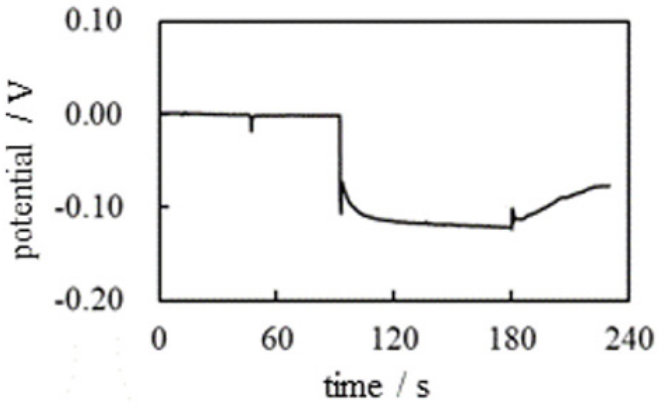

Figure 5: Exp.2 Time dependence of the potential between the indicator and the reference electrodes

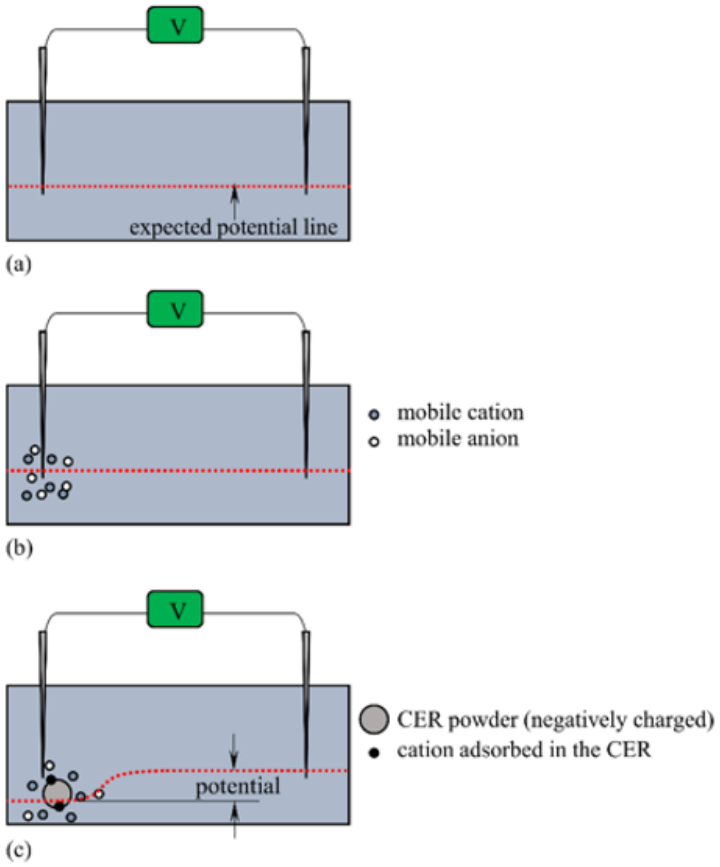

Figure 6: Exp.2 CER nearby the indicator electrode when (a) 0 s ≤ t ≤ 45 s, (b) 45 s ≤ t ≤ 90 s, (c) 90 s ≤ t ≤ 135 s "potential" suggested by two vertical arrows represents the experimentally measured potential.

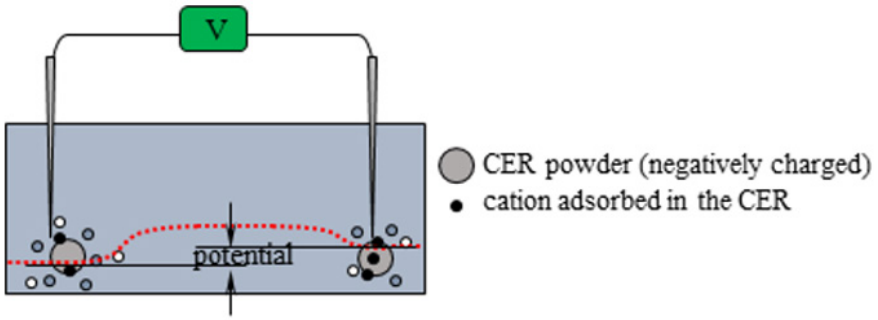

Figure 7: Exp.2 Potential profile change by the CER solution addition nearby the indicating electrode at t = 180 s "potential" suggested by two vertical arrows represents the experimentally measured potential.

Exp.3 Potential generated by the addition of Anion Exchange Resin

The same potential measurement as Exp.2 was performed according to the experimental procedure summarized in Table 4 where Anion Exchange Resin (AER) was used instead of CER, and the AER solution is the mixture of anion exchange resin (DOWE X, Cl form, Dow Chemical Company, Michigan, USA) and deionized water (see Figure 4). Figure 8 shows the potential versus time. There is no ion-selective membrane between the indicator and reference electrodes. However, the positive potential was clearly observed after t = 90 s. This nonzero potential cannot be explained by the membrane theory as no membranes are used in this potential measurement. However, these potential characteristics can easily be explained by the same cause as Exp.2 as follows: There were K^+ and

Cl^- near the indicator electrode after t = 45 s (see Figure 9). The total charge of K^+ and Cl^- is zero, and they are in thermal motion state. Consequently, the potentials generated by the individuals cancel out, resulting in a zero potential up to t = 90 s. However, the AER solution added in the vicinity of the indicator electrode at t = 90 s dissociates into a mobile anion and an immobile cation, as shown in Figure 9(c). The non-zero potentials generated by these mobile anions are largely canceled out by the potentials of all other mobile cations in thermal motion. However, the positive charges of the AER are virtually immobile, which explains why the positive potential is generated in the vicinity of the indicator electrode. That is, ion adsorption (or desorption) governs potential generation as the AIH states.

Table 4: Procedure of potential measurement.

t†1 / s	operation†2
0	onset time of the potential measurement
45	addition of a few drops of 10^{-4} M KCl solution near the indicator electrode
90	addition of a few drops of AER solution†3 near the indicator electrode.
135	addition of a few drops of 10^{-4} M KCl solution near the reference electrode
180	addition of a few drops of AER solution†3 near the reference electrode

† 1 t: time

† 2 The solution in the container of the set-up (see Figure 2) is a deionized water.

† 3 AER solution: The mixture of AER and deionized water.

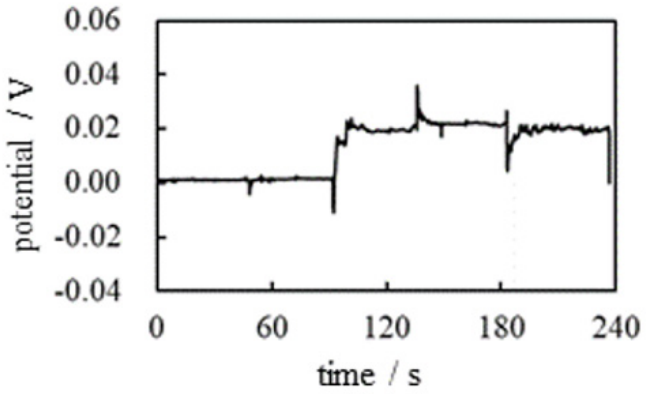

Figure 8: Time dependence of the potential between the indicator and the reference electrodes.

The potential was 0.02 V from t = 90 s to t = 180 s. When the AER solution was added close to the reference electrode at t = 180 s, the potential suddenly decreased. This phenomenon can be explained by the same cause as the increase in potential at t = 90 s. In fact, the decrease in potential at t = 180 s is due to the immobile positive charges of the AERs added in the vicinity of the reference electrode, as illustrated in Figure 10. But the potential gradually increases, reaching around 0.02 V at t = 190 s. This must be due to the dispersion of AER. That is, the potential plunged just after the addition of AER solution at t = 180 s, but the AER particles dispersed and their influence on the potential was unable to reach the reference electrode. Furthermore, the AER must be largely neutralized by mobile anions. Consequently, the potential gradually returned to around 0.02 V after t = 190 s. In this connection, we would like to show an experimental result in the section **Potential generated by the CER and AER**. Potential profiles caused by adding a CER (AER) solution in Exp.2 (Exp.3) are fully understandable from an electromagnetism point of view. Before showing the experiments in section **Potential in PVA aqueous solution** we would like to perform a simple theoretical analysis as follows: Let us consider the simplest analytical case of a solution potential in which immobile charges are surrounded by mobile ions. Imagine a plate that contains immobile functional atomic groups –COOH. Once this plate is immersed in an electrolytic solution, a certain amount of –COOH dissociates and the plate carries negative charges of $-COO^-$ (see Figure 11). This system was discussed in an earlier work by H.T. (one of the authors of this paper) [4,5]. Plate surface charge density, σ , and surface potential, ϕ , are associated with each other by Eq. 2.

The derivation process of Eq. 2 is shown in the references. [4] and [5] where ϵ: relative permittivity of water, $\in_0$: dielectric constant of vacuum, Q_0 : ion concentration in the bulk phase, k : Boltzmann constant, T : temperature, e: elementary charge and $\beta \equiv e/2kT$. Eq. 2 conforms to the Boltzmann distribution of ions and guarantees macroscopic electroneutrality. Consequently, the full contribution of ions to potential generation is taken into account in Eq. 2 thermodynamically.

$$\sigma = 2\sqrt{2 \in \in_0 Q_0 kT}\sinh(\beta\phi) \quad (2)$$

σ is negative due to the negative charge of $-COO^-$, and and $\epsilon, \epsilon_0, Q_0, k, T$ and e are positive quantities . Hence, ϕ of Eq. 2 is negative. Therefore, the negative immobile charge of CER can generate a negative potential and is clearly seen in Figure 5. Similarly, the positive immobile charge of AER can generate positive potential and is clearly seen in Figure 8.

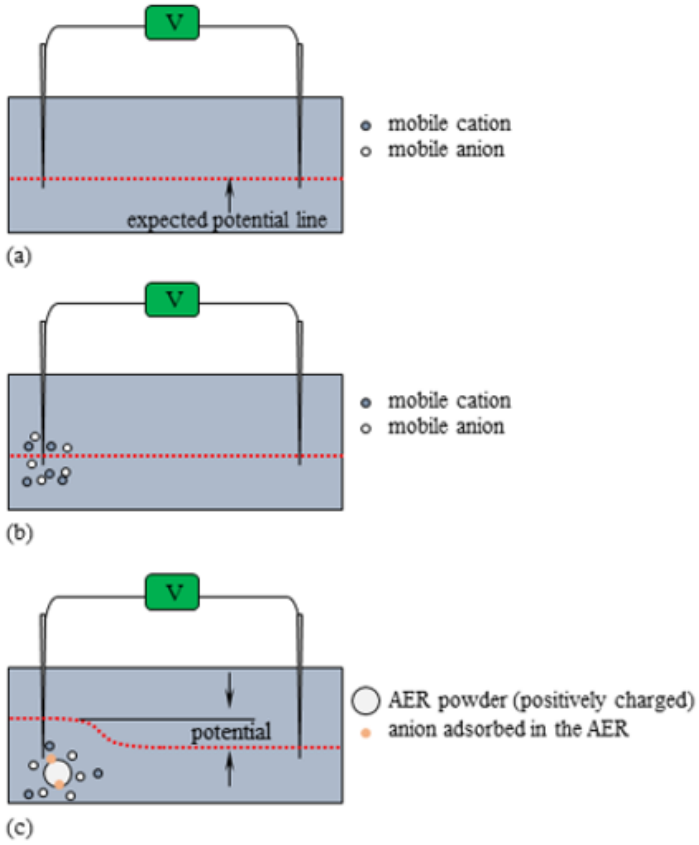

Figure 9: AER nearby the indicator electrode when (a) 0 s ≤ t ≤ 45 s, (b) 45 s ≤ t ≤ 90 s, (c) 90 s ≤ t ≤ 135 s "potential" suggested by two vertical arrows represents the experimentally measured potential.

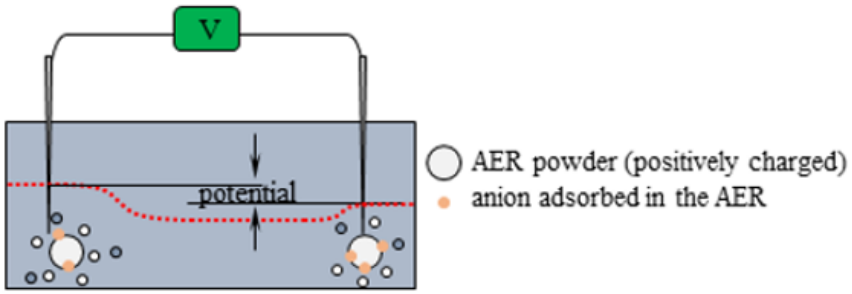

Figure 10: Potential profile change by the AER solution addition nearby the indicator electrode at t = 180s "potential" suggested by two vertical arrows represents the experimentally measured potential.

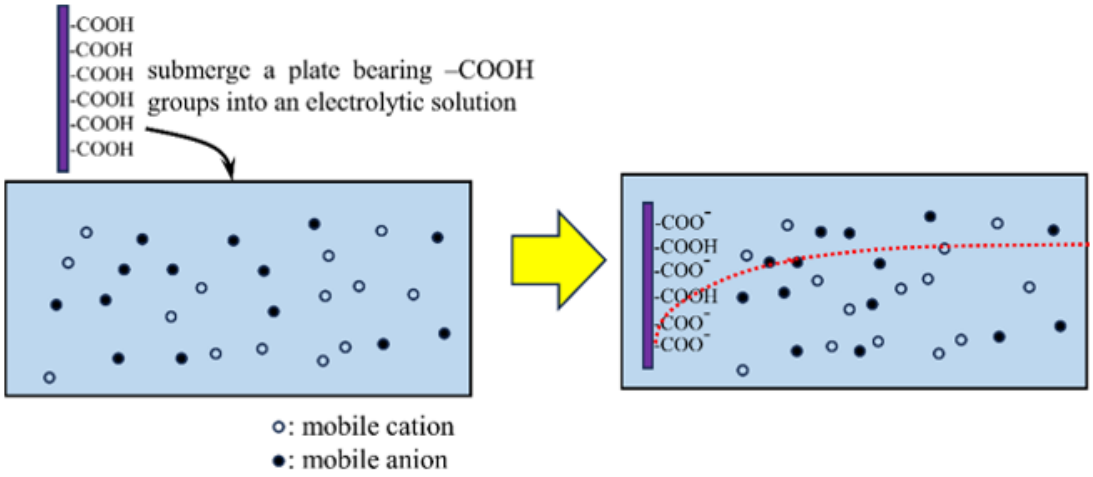

Figure 11: A plate bearing −COOH groups is submerged into an electrolytic solution. Due to the negative charges generated by the dissociation of −COOH, the potential profile represented by the dotted line is expected. The surface potential of this plate is negative by defining the bulk phase solution potential as zero.

Potential generated by the CER and AER

We prepared a 10^{-4} M KCl solution in petri dish in which a tiny amount of ion exchange resins (IER), CER and AER, was placed as illustrated in Figure 12. Then, the potential between the two electrodes was measured by changing the gap of the electrodes, x cm. The position of the reference electrode was fixed while the position of the indicator electrode was moved from x = 6.5 cm to 1.5 cm and then returned to x = 6.5 cm. The result is given in Figure 13. Figure 13 obviously suggests that the potential depends on the IER species (CER or AER) near the reference electrode and the distance between the IER and the reference electrode. To be precise, the potential profiles shown in Figs. 5 and 8 are strongly influenced by the distance between the indicator electrode and the IER (CER or AER). Consequently, sometimes the potential cannot be kept constant, as observed in Figure 8 after t = 180 s. The significant potential drop was induced at t = 180 s. But it gradually became nullified by t = 190 s, since the widening the gap between the AER and the reference electrode tip took place over time due to the AER dispersion.

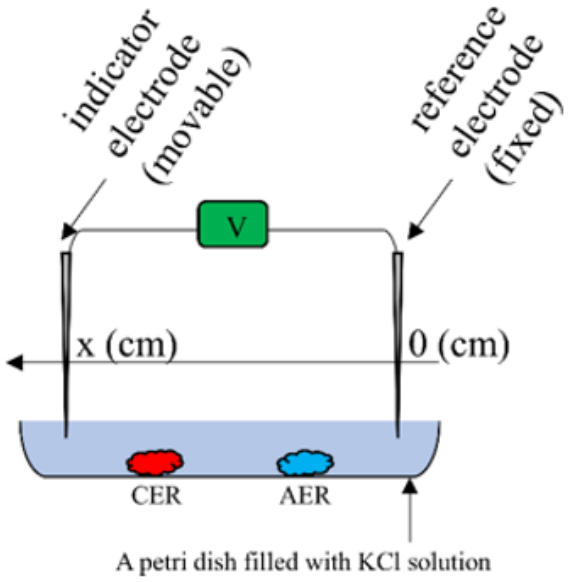

Figure 12: Experimental setup for measuring the KCl solution potential in the presence of CER and AER Be aware that the direction of x-axis is in the left.

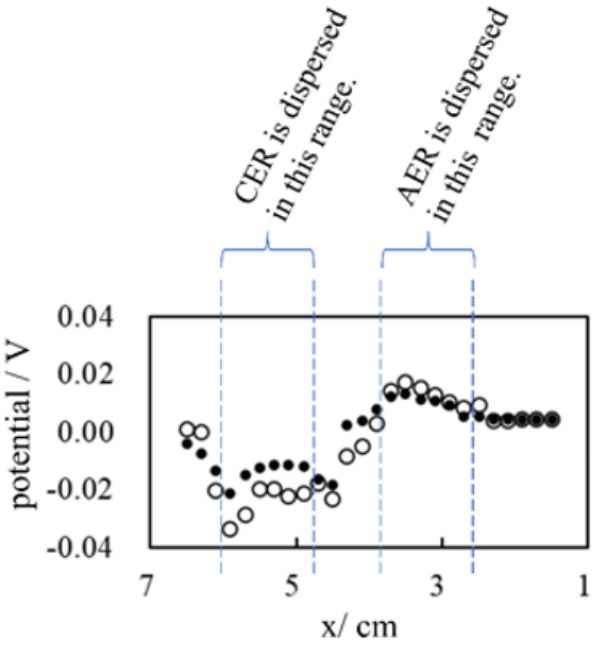

Figure 13: Potential between the indicator and the reference electrodes vs. the gap between the electrodes (x cm) in the presence of CER and AER The indicator electrode moves from x = 6.5 cm to 1.5 cm (○), then it returns from x = 1.5 cm to x = 6.5 cm (●)

Potential in PVA Aqueous Solution

The same potential measurement as described in Section 4.1 was performed here in the presence of a 16 wt% PVA aqueous solution. The experimental setup is the same as that illustrated in Figure 2, but the 16 wt% PVA aqueous solution was used instead of deionized water. The aqueous solution of PVA is highly viscous and is an appropriate material for the simulation of the protoplasm.

Exp.4 Potential Generated by the Addition of KCl Solution in the PVA Aqueous Solution

The container of the experimental setup was filled with the 16 wt% PVA aqueous solution. The potential generated between the two electrodes was measured as a function of time following the experimental procedure in Table 5. Figure 14 shows the time dependence of the potential generated between the indicator and the reference electrodes under the experimental conditions in Table 5. Although a momentary disturbance of the potential was observed when the KCl solution was dropped near the electrodes, the potential remained basically at 0 V. According to membrane theory, selective ion transport across the plasma membrane is responsible for generating a non-zero membrane potential. In this experiment, no ion-selective membrane was used. Therefore, the generation of a nonzero potential cannot be expected, and the experimental observation of the zero potential in Figure 14 is in perfect agreement with membrane theory. But as mentioned earlier in the section **Exp.1 Potential generated by the addition of KCl solution** no ion adsorption inevitably results in the zero potential by the AIH as well.

Table 5: Procedure of potential measurement.

t†1 / s	operation†2
0	onset time of the potential measurement
45	addition of a few drops of 10^{-4} M KCl solution near the indicator electrode
90	addition of a few drops of 10^{-1} M KCl solution near the indicator electrode
135	addition of a few drops of 10^{-4} M KCl solution near the reference electrode
180	addition of a few drops of 10^{-1} M KCl solution near the reference electrode

† 1 t: time

† 2 The solution in the container of the set-up (see Figure 2) is a 16 wt% PVA aqueous solution.

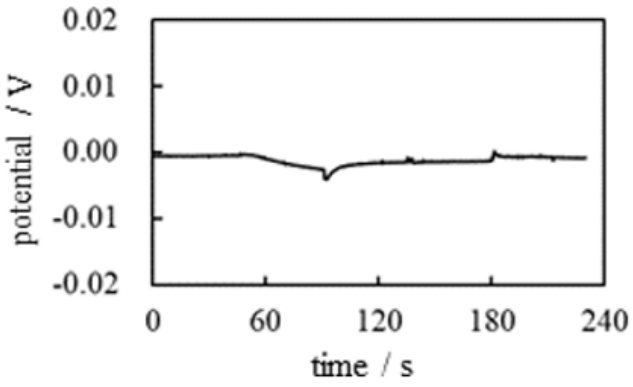

Figure 14: Exp.4 Potential between the indicator and the reference electrodes vs.time A 16 wt% PVA aqueous solution is used.

Exp.5 Potential Generated by the CER

The same potential measurement as Exp.2 was carried out. The experimental procedure was basically the same as in Table 3 but the container of the experimental setup was filled with a 16 wt% aqueous PVA solution in place of deionized water. The solid line in Fig. 15 shows the potential vs. time of Exp.5. The potential profile of Exp.5 in Figure 15 is to be analyzed step by step as follows: From t = 0 to 45 s, the potential is 0 V. This is normal and nothing to mention. From t = 45 to 90 s, no change in potential was induced, even with the addition of a 10^{-4} M KCl solution near the indicator electrode. This potential characteristic is also quite natural, since the electroneutrality of the K^{+} and Cl^{-} ions applies in this system and no ion-selective membrane is used in this system. However, the addition of CER solution in the vicinity of the indicator electrode at t = 90 s induced an abrupt drop in potential. This drop in potential cannot be explained by the membrane theory since there are no ion-selective membranes in this experimental system. However, the use of common electromagnetism may explain this. Indeed, the interpretation used in Exp.2 can be applied to this experiment Exp.5, that is, the immobile negative charge of the CER generated a nonzero negative potential. A slow and continuous decrease in potential was observed from t = 90 s to t = 135 s. This must be a slow process of descent of the CER solution from the aqueous surface of PVA to the bottom of the Petri dish where the tip of the indicator electrode was inserted (see Figure 16). The CER solution droplets from the pipette slowly reached the tip of the indicator electrode because of the high viscosity of the PVA aqueous solution, resulting in a slow decrease in potential.

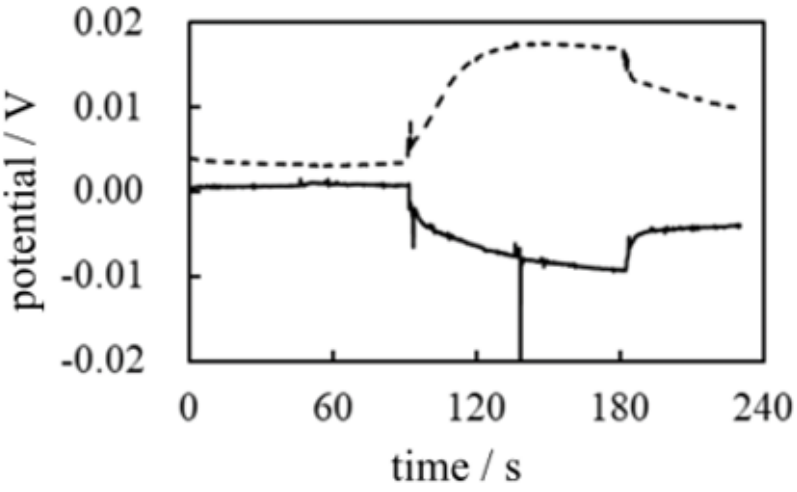

Figure 15: Exp.5 & Exp.6 Potential between the indicator and the reference electrodes vs. time A 16 wt% PVA aqueous solution is used.
Solid line: Exp.5 Dotted line: Exp.6

The addition of a 10^{-4} M solution of KCl in the vicinity of the reference electrode at t = 135 s caused virtually no discontinuous change in the downward potential trend. The steady and continuous decrease in potential continued until t = 180 s. However, the addition of CER in the vicinity of the reference electrode at t = 180 s triggered a discontinuous change in potential. This potential change is due to the same reason as the potential change observed at t = 90 s.

To sum up, the potential generation does not require an ion-selective permeable membrane, but a heterogeneous spatial charge distribution by the CER bearing the immobile charges. These charges involve the ion desorption/desorption characteristics which governs the potential characteristics is necessary for nonzero potential generation, and this must be the mechanism of membrane potential generation. This mechanism is in harmony with the AIH described in the section **Association-Induction Hypothesis (AIH)**.

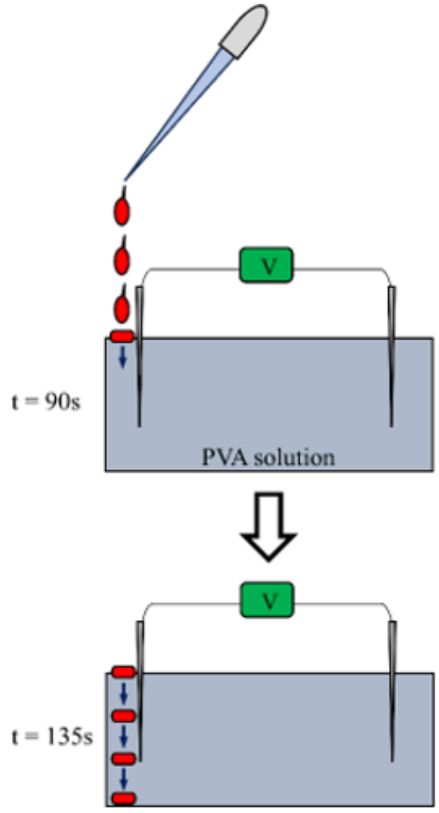

Figure 16: CER dropped from the tip of the pipette in the process of sinking from the surface of PVA aqueous solution to the petri dish bottom where the tip of the indicator electrode is placed.

Exp.6 Potential Generated by the AER

The same potential measurement as Exp.3 was performed. The experimental procedure was basically the same as in Table 4, but the solution that filled the container was the 16 wt% PVA aqueous solution in place of the deionized water. The dotted line in Figure 15 shows the potential vs. time of Exp.6. The potential profile of Exp.6 in Figure 15 is virtually opposite to that Exp.5 in Figure 15 about the x-axis. This is due to the use of the AER solution instead of the CER solution, namely, the sign of a fixed charge of AER is opposite to that of the CER. Therefore, such an opposite potential profile in Figure 15 is basically explicable by the use of the same discussion employed for Exp.5 with the opposite charge of AER in mind.

Potential Across a Membrane Separating two Solutions

It is well-known that the potential across an Ion Exchange Membrane (IEM) separating two electrolyte solutions is theoretically predictable quantitatively using the membrane theory. Let us imagine that two KCl solutions are separated by an anion exchange membrane that is largely permeable to anions but not very permeable to cations; Figure 17 roughly illustrates such a system. The GHK eq. is a well-known physiological equation that has been widely used to predict the membrane potential of a living cell. The GHK eq. is even applicable to nonliving systems such as the one shown in Figure 17. Tamagawa (one of the authors of this article) and Morita previously performed potential measurements across an anion-exchange membrane separating two KCl solutions and

found that the measured potentials obeyed the GHK eq. [55]. If the membrane theory is correct, then selective ion transport across the ion exchange membrane should have taken place in the experiment. Thus, the diffusion of ions across the membrane is necessary for the generation of the membrane potential. For further discussion, we would like to further explain the GHK eq. hypothesizing that the membrane theory is valid, although Tamagawa and Morita concluded that the potential they measured was caused by the heterogeneous spatial ion distribution caused by the adsorption of ions onto the membrane rather than by transmembrane ion transport [55].

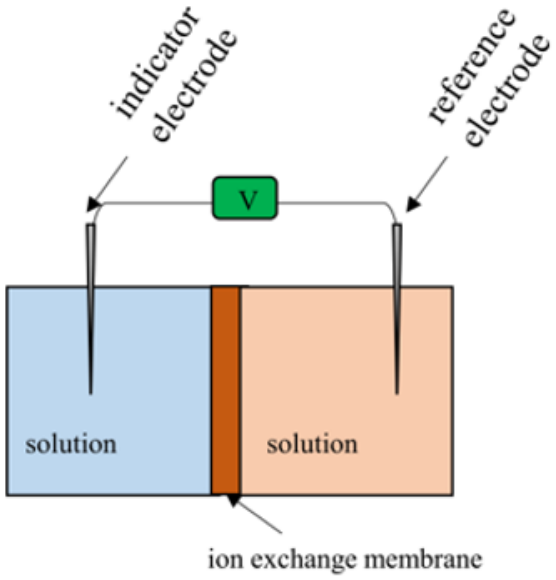

Figure 17: Experimental setup for measuring the potential between the two electrolytic solutions separated by a permeable ion exchange membrane.

Imagine that the two KCl solutions are separated by an ion exchange membrane (IER) as shown in Figure 17 and that the ion exchange membrane used is a cation exchange membrane. Its permeability to K^+ is much higher than that to Cl^-. In this case, the membrane potential is given by Eq. 3. Denoting membrane permeability at K^+ and Cl^- by P_k and P_{Cl} respectively, and denoting the concentrations of ions in the left and right phases by $[i]_L$ and $[i]_R$ ($i = K^+, Cl^-$), respectively, Eq. 3 is derived using the GHK equation. Since the membrane permeability to K^+ is much greater than to Cl^-, Eq. 5 is derived. Thus, Eq. 3 can be approximated by Eq. 4. Now, if the cation exchange membrane is replaced by an anion exchange membrane, what are the characteristics of the potential? The anion exchange membrane is highly permeable to the anion Cl^-, but not very permeable to K^+. Consequently, Eq. 6 is derived, and the GHK equation for this system can be given by Eq. 7, which gives Eq. 8. Since Eqs. 9 and 10 are valid, Eq. 11 is derived, that is, the cation or anion for which membrane permeability is higher determines the sign of the potential [56]. With the discussion described so far in this section, we will show another experiment in the following sections.

$$\phi_K = -\frac{kT}{e}\ln\frac{P_K\left[K^+\right]_L + P_{Cl}\left[Cl^-\right]_R}{P_K\left[K^+\right]_R + P_{Cl}\left[Cl^-\right]_L} \tag{3}$$

$$\sim -\frac{kT}{e}\ln\frac{P_K\left[K^+\right]_L}{P_K\left[K^+\right]_R} = -\frac{kT}{e}\ln\frac{\left[K^+\right]_L}{\left[K^+\right]_R} \tag{4}$$

$$P_K >> P_{Cl} \tag{5}$$

$$P_K << P_{Cl} \tag{6}$$

$$\phi_{Cl} = -\frac{kT}{e}\ln\frac{P_K\left[K^+\right]_L + P_{Cl}\left[Cl^-\right]_R}{P_K\left[K^+\right]_R + P_{Cl}\left[Cl^-\right]_L} \tag{7}$$

$$\sim -\frac{kT}{e}\ln\frac{P_{Cl}\left[Cl^-\right]_R}{P_{Cl}\left[Cl^-\right]_L} = -\frac{kT}{e}\ln\frac{\left[Cl^-\right]_R}{\left[Cl^-\right]_L} \tag{8}$$

$$\left[K^+\right]_L = \left[Cl^-\right]_L \tag{9}$$

$$\left[K^+\right]_R = \left[Cl^-\right]_R \tag{10}$$

$$\phi_K = -\frac{kT}{e}\ln\frac{P_K\left[K^+\right]_L}{P_K\left[K^+\right]_R} = -\frac{kT}{e}\ln\frac{\left[Cl^-\right]_L}{\left[Cl^-\right]_R}$$
$$= -\left(-\frac{kT}{e}\ln\frac{\left[Cl^-\right]_R}{\left[Cl^-\right]_L}\right) = -\phi_{Cl} \quad (11)$$

Exp.7 Potential Across an IEM Generated by the Addition of AER

The potential across the ion exchange membrane (IEM) was measured using the experimental setup identical to the illustration in Figure 17, but two 16 wt% aqueous PVA solutions were used instead of the two electrolyte solutions. We followed the procedure given in Table 6. Note that KCl solutions and IER solutions were dropped close to the indicator electrode and never dropped in the vicinity of the reference electrode, unlike the other experiments presented so far. The IER solutions used in this experiment were AER and CER, which are the same as those used in the experiments described earlier. The IEMs used were Selemion AMV and Selemion CMV (Asahi Glass, Co. Ltd. Tokyo) shown in Figure 18. Selemion AMV is an anion exchange membrane that bears fixed positive charges, whereas the Selemion CMV is a cation exchange membrane that bears fixed negative charges. Henceforth, Selemion AMV and Selemon CMV will be referred to simply as AMV and CMV, respectively.

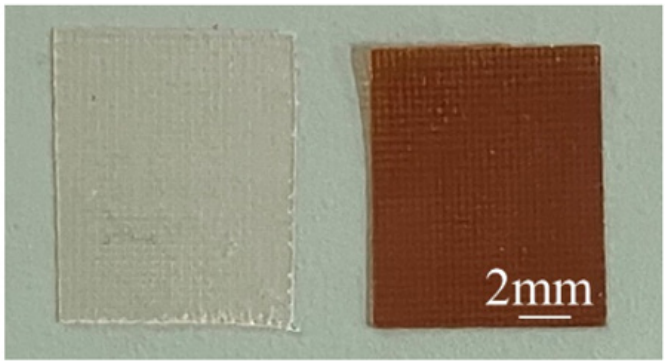

Figure 18: Ion Exchange Membranes (IEM) Left: Selemion AMV Right: Selemion CMV.

Since AMV is positively charged, it must be much more permeable to mobile anions than to mobile cations. On the other hand, CMV must be far more permeable to mobile cations than to mobile anions because the CMV is negatively charged. Consequently, the sign of the membrane potential across the AMV must be opposite to that across the CMV according to the discussion made using Eqs. 4 ~ 11 as long as the membrane theory is valid.

Table 6: Exp.7 (Exp.7-1 ~ Exp.7-4) Procedure of potential measurement across an IEM †1

t†2 / s	operation†3
0	onset time of the potential measurement
45	addition of a few drops of 10^{-1} M KCl solution near the indicator electrode
90	addition of a few drops of IER solutio†4 near the indicator electrode

† 1 IEM: Ion Exchange Membrane (AMV = anion exchange membrane that has positive charges, CMV = cation exchange membrane bearing negative charges)

† 2 t: time

† 3 Two solution are the 16 wt% PVA aqueous solutions.

† 4 IER solution: Ion Exchange Resin solution (AER solution, CER solution)

Exp.7-1 Potential across AMV caused by AER We carried out the potential measurement following the procedure shown in Table 6 under the conditions of using AMV as IEM and AER as IER. The solid line in Figure 19 represents the experimental curve of the potential data. 10^{-1} M KCl was added in the vicinity of the indicator electrode at t = 45 s, but it did not cause such an obvious change in potential and virtually no change in potential was induced. Assuming that the membrane theory is correct, this phenomenon can be interpreted as the fact that Cl^- could not cross the AMV since Cl^- could not reach the AMV due to the high viscosity of the PVA aqueous solution. However, once the AER solution was added in the vicinity of the indicator electrode at t = 90 s, the potential immediately plunged and began to increase. Of course, it is unlikely that mobile ions would reach the AMV so quickly because of the high viscosity of PVA aqueous solution. This experimental finding indicates that ion movement through the membrane does not play a role in the creation of the membrane potential. AMV has nothing to do with the generation of the membrane potential and that the heterogeneous distribution of ions resulting from the immobile charge of the AER is responsible for the generation of the membrane potential, as suggested by the AIH. The potential drop at t = 90 s is a fluctuation due to the momentary collision between the aqueous solution of PVA and the AER solution. However, after a while, this fluctuation gradually subsided and the potential began to increase because of the immobile positive charge of the AER solution.

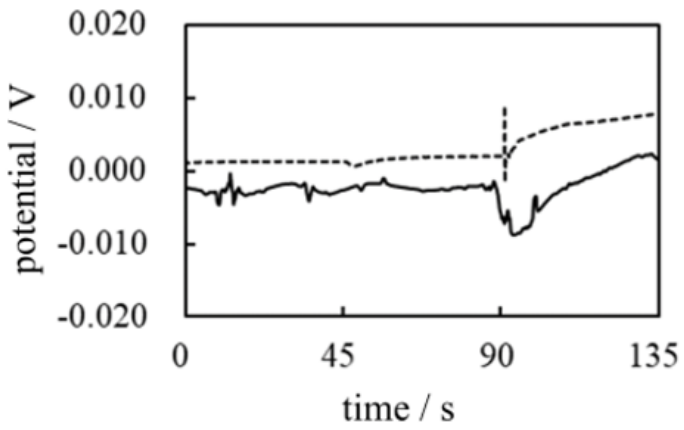

Figure 19: Exp.7-1 & Exp.7-2 Change of membrane potential across the IER caused by the addition of AER Solid line: Exp.7-1, An AMV was used as an IEM. Dotted line: Exp.7-2, A CMV was used as an IEM.

Exp.7-2 Potential across CMV caused by AER The same potential measurement as Exp.7-1 in Figure 19 was performed using the CMV in place of the AMV while the IER used was the AER which is the same type of IER used in the Exp.7-1. The CMV carries negative charges whose sign is opposite to that of the charge carried by the AMV. Consequently, the CMV must be highly permeable to K^+ and only slightly permeable to Cl^-. Therefore, the potential change expected by the addition of AER at t = 90 s is the decrease in potential assuming that the membrane theory is correct. The actual membrane potential observed is given by the dotted curve in Figure 19. In contrast to the expected potential profile, the actual observed potential showed an increase at t = 90 s by adding the AER solution. Consequently, this experimental result confirms the hypothesis that the heterogeneous ion distribution caused by the immobile charge of the AER is responsible for the generation of the membrane potential, as suggested by the AIH.

Exp.7-3 Potential across AMV caused by CER The same potential measurement was again carried out following the procedure shown in Table 6, with the provision that AMV was used as IEM and CER solution was used as the IER solution in place of AER solution. If the membrane theory is correct, the expected potential change should exhibit an increasing potential, which is the same potential trend as Exp.7-1 in which the AMV was used (see the solid line data curve of Exp.7-1 in Figure 19). On the other hand, if the heterogeneous ion distribution is responsible for generating the membrane potential, the potential must start to decrease with the addition of CER, since the sign of the immobile charge of CER is opposite to that of AER used in both Exp.7-1 and Exp.7-2. The actual potential profiles of Exp.7-1 and Exp.7-2 in Figure 19 exhibit the increase with the addition of the AER solution regardless of the type of IERs used. The actual trend in potential for Exp.7-3 is a decrease as represented by the solid line in Figure 20. This strongly confirms that the membrane potential is generated by the heterogeneous ion distribution due to ion adsorption and not by membrane theory.

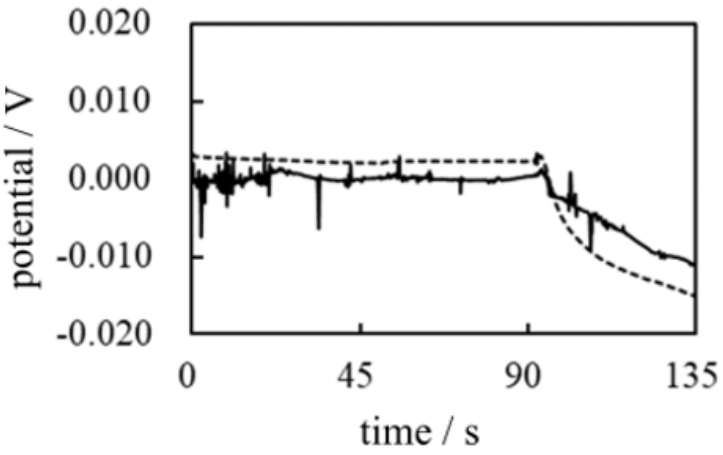

Figure 20: Exp.7-3 & Exp.7-4 Change of membrane potential across the IER caused by the addition of CER Solid line: Exp.7-3, An AMV was used as an IEM Dotted line: Exp.7-4, A CMV was used as an IEM.

Exp.7-4 Potential across CMV caused by CER The same potential measurement was again carried out following the procedure shown in Table 6, with the provision that the CMV was used as the IEM and the CER solution as the IER solution. As can be easily expected from the above discussion, the potential change occurs at the time when the CER solution was added, t = 90 s, while no potential change is expected only by adding the KCl solution at t = 45 s. In fact, the dashed potential profile in Figure 20 represents the experimentally measured potential for Exp.7-4 and is in full agreement with the expected potential profile based on AIH. Therefore, the membrane potential of living cells must be caused by the heterogeneous spatial distribution of ions (charge) through the ion adsorption.

Potential Characteristics in a Realistic Living Cell Model

On the basis of the experimentally observed potential characteristics and the discussions so far described, the spatial charge distribution resulting from the adsorption/desorption of mobile ions onto immobile charges plays a fundamental role in generating the membrane potential. This is fully in line with the AIH. In fact, a living cell contains many charged substances, such as lipids and proteins, and the adsorption of mobile ions onto these substances is inevitable. With this in mind, we focused on a more realistic model of a living cell and carried out measurements of its potential.

Potential in a Charged Solution in the Absence of a Membrane

Exp.8 Potential Generated in the Gelatin Aqueous Solution

An illustration of an experimental setup was used in Figure 2, but 16 wt% gelatin aqueous solution was poured into it. The gelatin aqueous solution used is charged and has a highly viscous protoplasm. Therefore, the aqueous solution of gelatin is a quite suitable model for a living cell. Using this experimental system, the potential measurement was carried out following the procedure in Table 7.

The 16 wt% gelatin aqueous solution is a highly viscous charged solution. Therefore, the fixed charges of the gelatin molecules are practically immobile, and their counterions are the mobile ions. Figure 21 illustrates the macroscopic particles of IER in an aqueous solution and a viscous solution highly congested with the gelatin molecules. IER particle dimension is the macroscopic level as illustrated in Figure 4. The charges on the IER particles are in the immobile state. Gelatin solution 16 wt% gelatin aqueous solution is highly viscous. Therefore, the motion of gelatin molecules is significantly restricted. Therefore, the charges on the gelatin molecules are virtually immobile. Once deionized water or 10^{-1} M KCl solution is poured into the 16wt% gelatin aqueous solution, the degree of dissociation of the gelatin molecule can be affected. This means that the degree of adsorption of ions on immobile charges will be altered. Therefore, a change in potential can be expected.

Figure 22 represents the potential measured experimentally according to the experimental procedure in Table 7. Although the potential change induced by the addition of deionized water at t = 45 s is unclear, the potential change induced by the addition of a solution of 10^{-1} M KCl at t = 90 s is quite clear. Consequently, AIH is strongly supported.

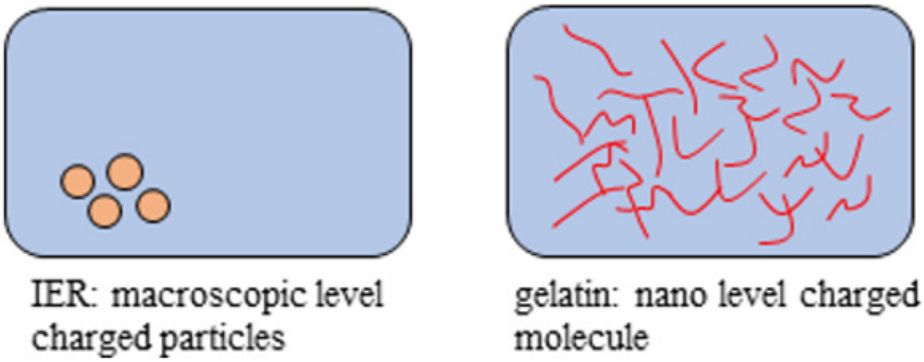

Figure 21: Immobile state Left: IER particles in a aqueous solution are in the immobile state Right: Gelatin molecules in the viscous solution state Gelatin molecules are virtually in the immobile state.

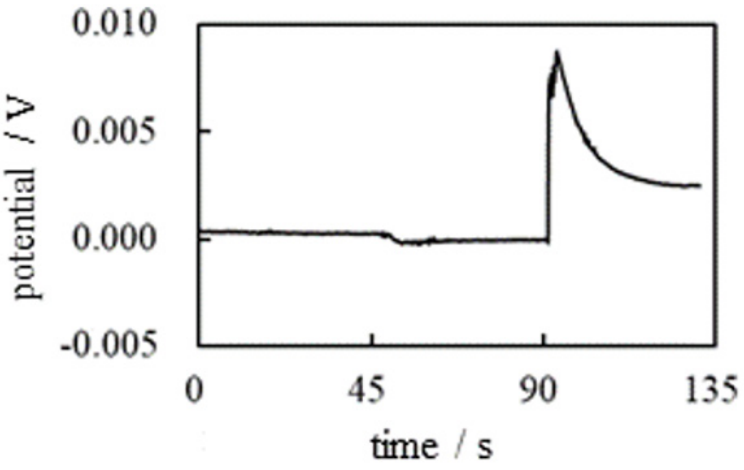

Figure 22: Exp.8 Potential generated in a gelatin aqueous solution vs. time.

Table 7: Exp.8 Procedure of potential measurement in a gelatin aqueous solution †1.

t†2 / s	operation
0	onset time of the potential measurement
45	addition of a few drops of deionized water near the indicator electrode.
90	addition of a few drops of 10^{-1} M KCl near the indicator electrode

†1 The solution is an aqueous 16 wt% gelatin aqueous solution.

†2 t: time

Exp.9 Potential Generated in the Aqueous Solution of PVA

For comparison, the same measurement as Exp.8 was carried out following the procedure in Table 7 using the 16 wt% PVA aqueous solution instead of the 16 wt% gelatin aqueous solution (note: this experiment is basically the same as Exp.4). The PVA aqueous solution is a neutral solution, unlike the gelatin aqueous solution. Consequently, no net change in potential can be expected from the addition of aqueous solutions.

Figure 23 shows the potential profile measured experimentally. Compared to the profile in Figure 22. It is no exaggeration to say that no potential change was induced from the beginning to the end. Therefore, the potential generation or the potential change must be induced by the spatial fixation of ions by the ion adsorption (or desorption) as suggested by the AIH.

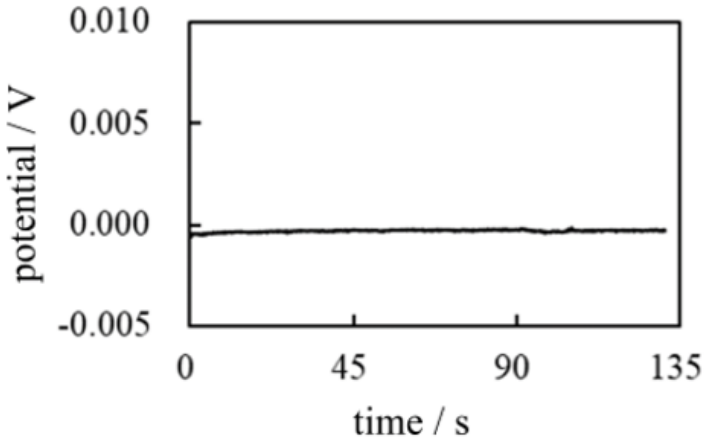

Figure 23: Exp.9 Potential generated in a PVA aqueous solution vs. time.

Potential in a charged solution across a membrane

Exp.10

The potential measurement was carried out using the setup illustrated in Figure 17 following the procedure in Table 7. The gelatin aqueous solutions were poured into both sides of a membrane in place of the electrolyte solution. The membranes used were an AMV and a CMV. As described above, the membrane does not play a fundamental role in potential generation. Consequently, regardless of which membrane is used, the potential characteristics should be fundamentally the same. In fact, the experimentally obtained potential profiles are fundamentally the same regardless of the membrane species used, as shown in Figure 24. Furthermore, this potential profile is quite similar to the potential profile of Figure 22 of Exp.8. Their similarity is quite understandable as long as the AIH is valid, since the AIH states that membrane permeability to ions does not contribute to membrane potential generation [1-3,53]. Namely, the experimental system of Exp.10 is the same as that of Exp.8 other than the presence / absence of the membrane.

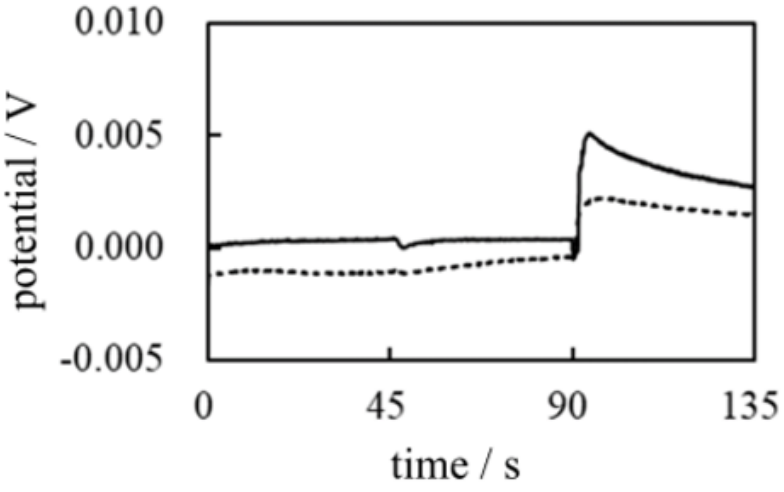

Figure 24: Exp.10 Potential generated across a membrane separating two gelatin aqueous solutions vs. time Solid line: potential across the CMV Dotted line: potential across the AMV.

Exp.11

The same potential measurement as Exp.10 was then performed using the procedure shown in Table 7, but in this experiment two types of solution were used instead of one. One is a gelatin aqueous solution, and the other is a PVA aqueous solution. A dialysis membrane was used as the membrane. Figure 25 illustrates the setup used for Exp.11. A dialysis membrane is impermeable to gelatin and PVA molecules but is permeable to K^+, Cl^- and water molecules, that is, the dialysis membrane (size 8, Wako, Japan) is not an ion-selective membrane.

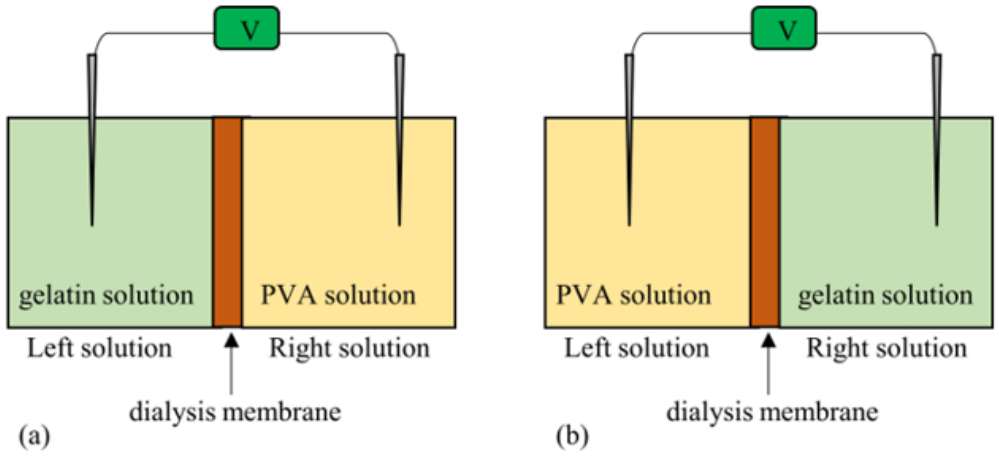

Figure 25: Setup for measuring the potential across a dialysis membrane separating a 16wt% gelatin aqueous solution and a 16wt% PVA aqueous solution (a) Left: 16wt% gelatin aqueous solution, Right: 16wt% PVA aqueous solution (b) Left: 16wt% gelatin aqueous solution, Right: 16wt% gelatin aqueous solution For both experimental systems shown in (a) and (b), the indicator electrode is always inserted in the Left solution while the reference electrode is always inserted in the Right solution.

Exp.11-1 Potential generated when the system in Figure 25(a) is used The potential profile is expected to be similar to Figure 22 since the addition of water at t = 45 s and the addition of 10^{-1} M KCl at t = 90 s are applied to the left aqueous solution of gelatin (containing immobile charges). As expected, a potential change was observed when the 10^{-1} M KCl solution was added at t = 90 s, as indicated by the solid line in Figure 26.

Exp.11-2 Potential generated when the system in Figure 25(b) On the other hand, the potential profile, when the system in Figure 25(b) is used, is expected to be similar to Figure 23 since the addition of water and 10^{-1} M KCl are performed in the left solution of PVA (electrically neutral molecule). As expected by AIH, the potential change was not observed even when the 10^{-1} M KCl solution was added at t = 90s, as indicated by the dotted line in Figure 26. Therefore, both profiles in Figure 26 are in line with the AIH prediction.

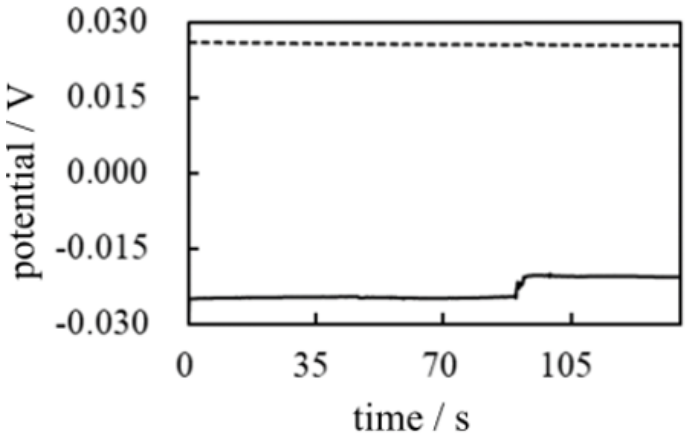

Figure 26: Exp.11 Potential generated across a dialysis membrane separating two solutions vs. time Solid line: Exp.11-1 (Left phase = 16wt% gelatin aqueous solution, Right phase = 16wt% PVA aqueous solution) Dotted line: Exp.11-2 (Left phase = 16wt% PVA aqueous solution, Right phase = 16wt% gelatin aqueous solution)

Viscous Nature of Living Cell and the Membrane Potential

Mobile ions cannot move as quickly through a viscous solution such as PVA and gelatin aqueous solutions. The same must apply to the living cell system. Consequently, mobile ions in the protoplasm cannot easily reach the inner surface of the plasma membrane. Therefore, transmembrane ion transport is not expected to occur with ease in living cells. Therefore, at least the fast change in membrane potential is an unimaginable event, although membrane theory attributes the generation of membrane potential in the living cell to transmembrane ion transport.

It can be argued that transmembrane ion transport occurs only in the vicinity of the plasma membrane, as illustrated in Figure 27. Thus, the viscous nature of the protoplasm does not affect the generation of the membrane potential. However, common theoretical treatments performed to estimate the membrane potential always relate to the entire cell body. For example, when the GHK equation is used to estimate cell potential, the local ion concentration is generally not taken into account, but the ion concentration in the entire cell is [6-8]. If transmembrane ion transport is to be considered a local event, much of the theoretical treatment for estimating the membrane potential must be reconsidered, even in the widely accepted membrane theory.

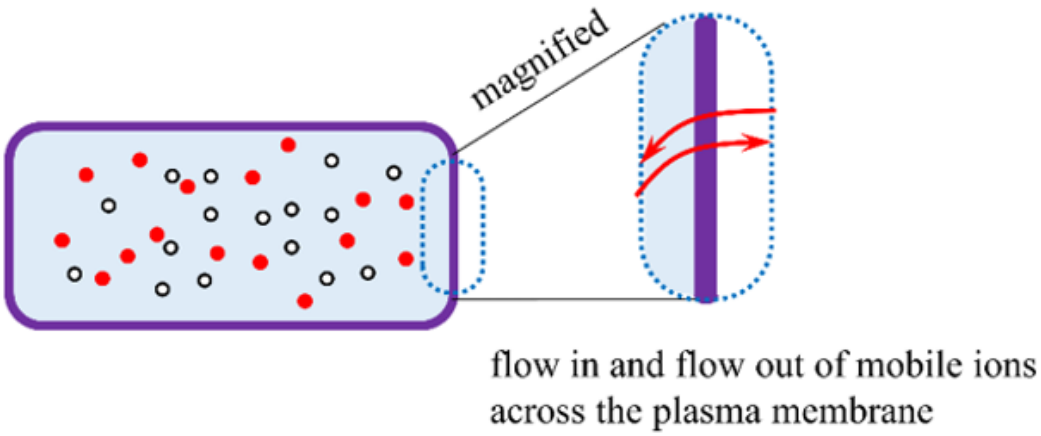

Figure 27: Illustration of the flow in and flow out of mobile ions across the plasma membrane.

Before moving on to the last section, we would like to touch on the reproducibility of the data of the experimentally measured potentials so far shown in this paper. In this work, we investigate the dynamic potential characteristics. It is not the potentials in the equilibrium state. The experimental procedure is basically as follows: A minute quantity of electrolytic solution (or ion-exchange resin particles) is manually dropped into a large amount of aqueous solution in a container using a pipette. The dropped electrolytic solution (or ion-exchange resin particles) disperses into the solution in the container randomly. Then, the potential induced in this solution was measured as a function of time. Since this dispersion process is a random process, not an equilibrium process, the quantitative reproducibility of the potential data cannot be expected. In fact, we could not observe the reproducibility of the quantitative potential data. It is a fairly natural consequence. However, we could repeatedly confirm that the reproducibility of the qualitative potential data is excellent. Therefore, our experimental data are reliable enough.

Conclusion

Living cells contain many charges of ions, lipids, and proteins. Therefore, it is quite natural to believe that these ions have more or less an effect on membrane potential generation. However, in membrane theory, which is the central concept of current physiology, the generation of membrane potentials has been attributed to the passage of mobile ions across the plasma membrane [1,2]. The influence of ion adsorption on the generation of membrane potential is completely missing. Physiologists sometimes consider ion adsorption in membrane potential investigation and even discuss the influence of charges, which can vary according to the degree of ion adsorption, on membrane potential [38,41,42]. However, such an influence of the charges created by the ion adsorption (and/or desorption) has never been incorporated into the commonly accepted membrane potential formula such as the GHK eq. as touched upon earlier. Somehow, the influence of ion adsorption on the membrane potential is not considered in current physiology when it comes to numerical calculation of the membrane potential. This work indicates that the ion adsorption (and/or desorption) plays a fundamental role for membrane potential generation and even indicates that the ion passage across the membrane has nothing to do with the membrane potential generation. This conclusion is in harmony with the long-forgotten physiological theory of AIH [1,2]. Although AIH is not accepted in the field of mainstream physiological sciences, we should not rule out AIH as a membrane potential generation mechanism. Through this work on the elucidation of the membrane potential generation mechanism, what is important for the pursuit

of genuine physiology in the future also emerges on its own. To pursue genuine physiology, we have to view the living cell in a more realistic way. For example, our experimental work described in this paper suggests that the viscous nature of protoplasm affects the characteristics of the electrolytic solution system in question and could drastically alter the individual ion characteristics. The diffusivity of the ions, their degree of adsorption/desorption, and their activities when they are in the viscous solution must be totally different from those of the ions in free water. In addition, the activity of water in the protoplasm must also be greatly diminished compared to that of free water [1,2]. In physical chemistry, it has even been known that the thermodynamical characteristics of the actual electrolytic solution are far from the ideal characteristics [57]. Physical chemists came to the theoretical tools, thermodynamics for the real system, to analyze these unideal characteristics of the actual electrolytic solution more than a half century ago [54]. Therefore, the unideal characteristics of electrolytic solution systems have been scrutinized in detail for many decades, and colloid chemistry is a typical example of the use of thermodynamics for the real system [48,58]. Colloid chemistry has revealed the unique characteristics of the mass of a long-hydrocarbon-chain molecule such as lipids, which are a component of the plasma membrane. The exhibition of the phase transition of the lipid bilayer is one of such characteristics. It is quite natural to believe that the dynamic characteristics of the membrane potential, in other words, the action potential, must be under the heavy influence of the phase transition of the plasma membrane [58-60]. Therefore, colloid chemistry could serve as a useful tool for analyzing the generation of action potentials. Furthermore, the thermodynamics of the real system can elucidate the genuine mechanism of functions of living cells, including the membrane potential generation mechanism. The Association-Induction Hypothesis must be a key concept for achieving it since its foundation lies in the view of seeing the living cell system realistically.

Author Contributions

Conceptualization, H.T.; methodology, H.T.; validation, H.T., B.D. W.L. and M.S.; formal analysis, H.T.; investigation, H.T. and B.D.; data curation, H.T.; writing-original draft preparation, H.T.; writing—review and editing, H.T., B.D. W.L. and M.S.

Funding

This research received no external funding.

Acknowledgement

None.

Conflicts of Interest

The authors declare no conflicts of interest.

References

1. Ling G N (1992) A Revolution in the Physiology of the Living Cell. Krieger Pub Co, Malabar, Florida.
2. Ling G N (2001) Life at the Cell and Below-Cell Level: The Hidden History of a Fundamental Revolution in Biology. Pacific Press, New York.
3. Ling G N (1997) Debunking the alleged resurrection of the sodium pump hypothesis. Physiol Chem Phys Med NMR 29(2): 123-198.
4. Tamagawa H, Ikeda K (2018) Another interpretation of Goldman-Hodgkin-Katz equation based on the Ling's adsorption theory. Euro Biophys J 47(8): 869-879.
5. Tamagawa H (2019) Mathematical expression of membrane potential based on Ling's adsorption theory is approximately the same as the Goldman–Hodgkin–Katz equation. J Biol Phys 45(1): 13-30.
6. Cronin J (1987) Mathematical aspects of Hodgkin-Huxley neural theory. Cambridge University Press, New York.
7. Keener J, Sneyd J (2008) Mathematical physiology: I: cellular physiology. Interdisciplinary applied mathematics. Springer, New York.
8. Ermentrout G B, Terman T H (2010) Mathematical foundations of neuroscience, vol 35. Interdisciplinary applied mathematics book. Springer, New York.
9. Lee JW (2020) Protonic conductor: better understanding neural resting and action potential. J Neurophysiol 124: 1029-1044.
10. M W Beaumont, E W Taylor, P J Butler (2000) The resting membrane potential of white muscle from brown trout (Salmo trutta) exposed to copper in soft, acidic water. The Journal of Experimental Biology 203(pt 14): 2229-2236.
11. Barry P H (2006) The Reliability of Relative Anion–Cation Permeabilities Deduced from Reversal (Dilution) Potential Measurements. Cell Biochem Biophys 46(2): 143-154.
12. Clay J R (2009) Determining K channel activation curves from K^+ channel K^+ currents often requires the Goldman–Hodgkin–Katz equation. Frontiers in Cellular Neuroscience 3: 20.
13. Navarro-Retamal C, Schott-Verdugo, S, Gohlke H, Dreyer I (2021) Computational Analyses of the AtTPC1 (Arabidopsis Two-Pore Channel 1) Permeation Pathway. International Journal of Molecular Sciences 22(19): 10345.
14. Powell C L, Brown A M (2021) A classic experiment revisited: membrane permeability changes during the action potential. Adv Physiol Educ 45(1): 178-181.
15. Forehand C J (2009) Synaptic Transmission, and Maintenance of Nerve Function. Medical Physiology: Principles for Clinical Medicine (Rhoades, R A; Bell, D R eds., Lippincott Williams & Wilkins, a Wolters Kluwer business. Philadelphia pp. 38-64.
16. O'Hara T, Virág L, Varró A, Rudy Y (2011) Simulation of the Undiseased Human Cardiac Ventricular Action Potential: Model Formulation and Experimental Validation. PLos Computational Biology 7(5): e1002061.
17. Alvarez O, Latorre R (2017) The enduring legacy of the "constant-field equation" in membrane ion transport. J Gen Physiol 149(10): 911-920.
18. Xie D (2022) An Extension of Goldman-Hodgkin-Katz Equations by Charges from Ionic Solution and Ion Channel Protein. arXiv:2208.11293.
19. Schwiening C J (2012) A brief historical perspective: Hodgkin and Huxley Protein. J Physiol 590(11): 2571-2575.
20. Ion and water transport . TIBS - October, 1977.
21. Edelman L (2005) DOUBTS ABOUT THE SODIUM-POTASSIUM PUMP ARE NOT PERMISSIBLE IN MODERN BIOSCIENCE. Cellular and Molecular Biology 51(8): 725-729.
22. Ishima Y, Przybylski A T, Fox SW (1981) Electrical membrane phenomena in spherules from proteinoid and lecithin. Biosystems 13(4): 243-251.
23. Przybylski A T, Stratten W P, Syren R M, Fox S W (1982) Membrane, action, and oscillatory potentials in simulated protocells. Naturwissenschaften 69(12): 561-563.
24. Przybylski A T, Fox S W (1984) Excitable artificial cells of proteinoid. Appl Biochem Biotechnol 10: 301-307.

25. Przybylski A T (1985) Excitable cell made of thermal proteinoids. Biosystems 17(4): 281-288.

26. Vaughan G, Przybylski A T, Fox S W (1987) Thermal proteinoids as excitability-inducing materials. Biosystems 20(3): 219-223.

27. Yoshikawa K, Matsubara Y (1983) Spontaneous oscillation of electrical potential across organic liquid membranes. Biophys Chem 17(3): 183-185.

28. Yoshikawa K, Sakabe K, Matsubara Y, Ota T (1984) Oscillation of electrical potential in a porous membrane doped with glycerol α-monoolate induced by an Na^+/K^+ concentration gradient. Biophys Chem 20(1-2): 107-109.

29. Yoshikawa K, Sakabe K, Matsubara Y, Ota T (1985) Self-excitation in a porous membrane doped with sorbitan monooleate (Span-80) induced by an Na^+/K^+ concentration gradient. Biophys Chem 21(1): 33-39.

30. Yoshikawa K, Omochi T, Matsubara Y, Kourai H (1986) A possibility to recognize chirality by an excitable artificial liquid membrane. Biophys Chem 24(2): 111-119.

31. Yoshikawa K, Omochi T, Matsubara Y (1986) Chemoreception of sugars by an excitable liquid membrane. Biophys Chem 23(3-4): 211-214.

32. Yoshikawa K, Shoji M, Nakata S, Maeda S (1988) An Excitable liquid membrane possibly mimicking the sensing mechanism of taste. Langmuir 4: 759-762.

33. Nakajo N, Yoshikawa K, Shoji M, Ueda I (1990) Spontaneous oscillation of artificial membrane: Equivalence in effects of temperature and volatile anesthetic. Biochem Biophys Res Commun 167(2): 450-455.

34. Flasterstein A H (1966) VOLTAGE FLUCTUATIONS OF METAL-ELECTROLYTE INTERFACES IN ELECROPHYSIOLOGY. Med & Engng 4(6): 583-588.

35. Flasterstein A H (1966) A GENERAL ANALYSIS OF VOLTAGE FLUCTUATIONS OF METAL-ELECTROLYTE INTERFACES. Med & Engng 4(6): 589-594.

36. Ling G N (1978) MAINTENANCE OF LOW SODIUM AND HIGH POTASSIUM LEVELS IN RESTING MUSCLE CELL. J Physiol 280: 105-123.

37. Tamagawa H, Ikeda K (2017) Generation of membrane potential beyond the conceptual range of Donnan theory and Goldman-Hodgkin-Katz equation. J Biol Phys 43(3): 319-340.

38. O Aono, S Oki (1972) Origin of Resting Potential of Axon Membrane. J Theor Biol 37(2): 273-282.

39. Jackson M B (2006) Molecular and Cellular Biophysics, Cambridge University Press, Cambridge.

40. Gutmann F, Keyzer H (1986) (Eds) Modern Bioelectrochemistry, Plenum Press, New York and London.

41. Benarroch J M, Asally M (2020) The Microbiologist's Guide to Membrane Potential Dynamics. Trends in Microbiology 28(4): 304-314.

42. Hughes M P (2024) The cellular zeta potential: cell electrophysiology beyond the membrane. Integrative Biology 16: zyae003.

43. Pollack G H (2001) Cells, Gels and the Engines of Life: A New, Unifying Approach to Cell Function, Ebner & Sons, Seattle, USA.

44. Pollack G H (2013) The Fourth Phase of Water: Beyond Solid, Liquid, and Vapor, Ebner & Sons, Seattle, USA.

45. G E Wnek (2016) Perspective: Do Macromolecules Play a Role in the Mechanisms of Nerve Stimulation and Nervous Transmission? JOURNAL OF POLYMER SCIENCE, PART B: POLYMER PHYSICS 54: 7-14.

46. Matveev VV (2017) Comparison of fundamental physical properties of the model cells (protocells) and the living cells reveals the need in protophysiology. Int J Astrobiol 16: 97-104.

47. Matveev VV (2019) Cell theory, intrinsically disordered proteins, and the physics of the origin of life. Progress in Biophysics and Molecular Biology 149: 114-130.

48. Bagatolli L A, Mangiarotti A, Stock R P (2020) Cellular metabolism and colloids: Realistically linking physiology and biological physical chemistry. Prog Biophys Mol Biol 162: 79-88.

49. Bagatolli L A, Stock R P (2021) Lipids, membranes, colloids and cells: a long view. BBA Biomembranes 1863(10): 183684.

50. Schneider M F (2021) Living systems approached from physical principles. Prog Biophys Mol Biol 162: 2-25.

51. Matveev V V (2022) Membraneless physiology of the living cell. The past and the present. 4 Open 5: 15.

52. Wnek G E, Costa A C S, Kozawa S K (2022) Bio-Mimicking, Electrical Excitability Phenomena Associated with Synthetic Macromolecular Systems: A Brief Review with Connections to the Cytoskeleton and Membraneless Organelles. Frontiers in Molecular Neuroscience 15: 830892.

53. Ling G N (2007) Nano-protoplasm: the Ultimate Unit of Life. Physiol Chem Phys & Med NMR 39(2): 111-234.

54. Lewis G N, Randall M (1961) Thermodynamics and the Free Energy of Chemical Substances. McGraw-Hill, NY.

55. Tamagawa H, Morita S (2014) Membrane Potential Generated by Ion Adsorption. Membranes 4(2): 257-274.

56. Tamagawa H, Mulembo T, Delalande B (2021) What can S-shaped potential profiles tell us about the mechanism of membrane potential generation? Membranes 50(6): 805-818.

57. Barrow G M (1984) Physical Chemistry, McGraw-Hill Inc., NY.

58. Israelachvili J N (1985) INTERMOLECULAR AND SURFACE FORCES With Applications to Colloidal and Biological Systems, Academic press, NY.

59. Matsuki H, Goto M, Tamai N (2019) Recent Progress in Biophysical Research of Biological Membrane Systems. Chem Pharm Bull 67: 300-307.

60. Fedosejevsa C S, Schneider M F (2022) Sharp, localized phase transitions in single neuronal cells. PNAS 119: e2117521119.